ρ_B = pellet density, g./cc.
ρ_p = particle density, g./cc.
ρ_t = solid density, gm./cc.
ϵ_a = macropore void fraction in a pellet
ϵ_i = micropore void fraction in a pellet
ϵ_{ip} = micropore void fraction in particle

Subscripts

1 = entrance of the reactor
2 = exit of the reactor

LITERATURE CITED

1. Jost, W., "Diffusion," Verlag Von Steinkopff, Darmstadt, Germany (1957).
2. Rao, M. Raja, N. Wakao, and J. M. Smith, "Diffusion and Reaction Rates for Ortho-hydrogen Conversion," submitted to *Ind. Eng. Chem.*
3. Robertson, J. L., and J. M. Smith, *A.I.Ch.E. Journal*, **9**, No. 3, p. 342 (1963).
4. Wakao, N., P. W. Selwood, and J. M. Smith, *A.I.Ch.E. Journal*, **8**, 478 (1962).
5. ————, J. M. Smith, and P. W. Selwood, *J. Catalysis*, **1**, 62 (1962).
6. Wakao, N., and J. M. Smith, "Diffusion in Catalyst Pellets," *Chem. Eng. Sci.*, **17**, 825 (1962).
7. ————, "Diffusion and Reaction Rates for Porous Catalysts," submitted to *Ind. Eng. Chem.*
8. Weitzel, D. H., and L. E. White, *Rev. Sci. Instr.*, **26**, 290 (1955).
9. Wheeler, Ahlborn, "Advances in Catalysis," Vol. 3, p. 250, Academic Press, New York (1950).
10. ————, "Catalysis," Vol. 2, p. 105, Reinhold, New York (1955).
11. Woolley, H. W., R. B. Scott, and F. G. Brickwedde, *J. Res. Nat'l Bur. Std.*, **41**, 379 (1948).

Manuscript received November 26, 1962; revision received April 1, 1963; paper accepted April 2, 1963.

A High Resolution Resistivity Probe for Determination of Local Void Properties in Gas-Liquid Flow

L. G. NEAL and S. G. BANKOFF

Northwestern University, Evanston, Illinois

Although considerable research has been devoted to the study of concurrent flow of gas—liquid or vapor—liquid mixtures, many details of the basic flow structure remain unknown. An important reason has been the lack of instrumentation capable of precise measurement of local parameters, such as local volumetric gas fraction, bubble frequency, and local bubble size distribution.

Most previous studies have used techniques which measured gas fractions averaged over the channel cross section. These methods employ the attenuation of gamma rays and beta rays (*1, 2, 3*); radioactive tracers (*4*); photographic records (*5*); and weighing a test section (*6*) The most popular of these is the gamma-ray technique, in which gamma rays from a radioactive source are passed through the stream. The strength of the attenuated beam is a function of the stream density and hence related to the gas fraction.

Hooker and Popper (*1*) have studied this method at some length and include an uncertainty analysis in their report. They concluded, from work with lucite mock-ups corresponding to gas concentrated at particular locations within the channel, that the gamma-ray technique was unsatisfactory for nonhomogeneous flow. Cook (*8*) and Egen (*7*) reported errors as large as 93% in annular flow. This source of error is common to all techniques which measure cross-sectional average gas fractions.

The gamma technique was improved by Petrick (*2*) who used a traversing method in which the source and detector were moved across the channel to get a gas fraction profile. The cross-sectional average gas fraction was obtained by integration of this profile. The advantage of the traversing technique is that an average is made over only one space coordinate; this reduces errors due to nonuniform gas distribution. Further, it gives a rough approximation to the gas fraction profile. The gamma-ray method is reasonably accurate for determining cross-section average gas fractions when the gas is uniformly distributed; the test section offers a radiation path greater than 1 in. of water, and the gas fraction is greater than 0.25. However, the method detects space-average rather than local values of the gas fraction and gives no information on individual bubble frequencies and size distributions. Recently radial void fractions have been obtained by the traversing technique with a polynomial-fitting procedure (*14*).

Several cases are reported in the literature of the use of probing techniques to measure local parameters in two-phase flow. Krasiakova (*9*) used a hot-wire anemometer to measure liquid film thickness in horizontal annular flow. McManus (*10*) used a precalibrated capacitance probe to measure the thickness of the liquid film for the same case. Hewitt (*11*) used a capacitance probe to measure film thickness in vertical flow. Both techniques were used to measure surface wave frequency and height. Solomon (*12*) has employed a conductivity probe as a flow regime indicator in air-water flow.

In this work an electrical resistivity probe is described which is capable of measuring local values of the volumetric gas fraction, bubble frequencies, and local bubble size spectra in a mercury-nitrogen system, where the output appears as a random square wave. Analysis of this signal in terms of autocorrelation functions and power density spectra is expected to provide valuable new information concerning the structure of two-phase flow.

DEFINITION OF TERMS

Before discussing the instrument, the variables to be measured should be clearly defined. Bubble frequency and bubble size distribution at a point are, respectively, the number of bubbles that pass through the point per unit

L. G. Neal is with the Norwegian Institute for Atomic Energy, Kjeller, Norway.

time, averaged over a suitably long time interval, and the diameter probability distribution function of these bubbles. Thus, the bubble frequency is

$$f = N/T \tag{1}$$

where f is the frequency in bubbles per second, and N is the total number of bubbles that pass through the point in time T. The time T must be a period of time long enough to obtain a representative sample which implies $N >> 1$.

The bubble size distribution is expressed as a cumulative bubble diameter distribution function $B(\zeta)$

$$B(\zeta) = \int_o^\zeta b(z)\, dz \tag{2}$$

where $z = D_B/D_P$ is a bubble diameter made dimensionless with reference to the pipe diameter, and $b(z)$ is a density function for bubbles of diameter z. The function $B(\zeta)$ is the probability that the diameter of an observed bubble will be less than ζ. Thus $B(a) = P(\zeta < a)$. In slug flow, the gas slug length and liquid slug length distributions are also important quantities for which cumulative distribution functions can be defined analogously to Equation (2).

For gas slugs

$$G(\zeta) = \int_1^\zeta g(z)\, dz \tag{3}$$

and for liquid slugs

$$L(\zeta) = \int_0^\zeta l(z)\, dz \tag{4}$$

where $G(\zeta)$ and $L(\zeta)$ are the gas slug length and liquid slug length cumulative distribution functions, respectively, and $g(z)$ and $l(z)$ are the corresponding density functions. The lower limits on the integrals (2.3) and (2.4) differ, since a gas slug is arbitrarily defined as a bubble for which $\zeta \geq 1$ while a liquid slug is defined as the liquid which separates two gas slugs and hence has no minimum size. In general, the liquid is not homogeneous but contains many small ($\zeta < 1$) gas bubbles.

In general, the point or local volumetric gas fraction (commonly called void fraction) may be defined as the probability that gas will exist at a particular point in the flow field at a particular time. For a stream with steady time-average properties (quasi-steady) this probability can be evaluated by averaging measurements at any point over a suitable time interval. If, in addition, the flow field is homogeneous, implying that the time-averaged properties are space-independent, one can replace the time average by a space average over some suitable volume. If the flow is not quasi-steady, the definition of homogeneity becomes more difficult. One may consider a local space-average property, which for a particular point at any instant may be identified as the mean property, such as void fraction of a spherical volume, chosen to contain a large number of bubbles, surrounding the point. In general, the radius of the sample sphere should be chosen, if possible, to be small compared to the scale of spatial variation of the local space-average properties. A homogeneous two-phase flow field is then defined as one for which the local space—average properties are independent of position. If the flow is neither quasi-steady nor homogeneous, an ensemble average at the point in space and time must be taken over a large number of experiments with the same initial and boundary conditions. For quasi-steady flow the gas fraction is therefore expressed as

$$\alpha = \frac{1}{T}\int_0^T [1 - \phi(t)]\, dt \tag{5}$$

where α is the volumetric gas fraction, and $\phi(t)$ is a discontinuous function of time that assumes the value of one when liquid exists at the point and of zero when gas exists at the point. As before, the time interval T must be large compared with the time scale of the flow oscillations, $1/f$. On the other hand, it must be small compared to any slow variations in the field of flow that are not to be associated with the instantaneous fluctuations.

PRINCIPLE OF OPERATION

The probe (Figure 1) consists of a 1.25-in. steel sewing needle welded to the end of a 6-in. length of 0.033-in. steel wire. The steel wire is electrically insulated and encased in a 3-in. length of ⅛-in. stainless steel tube .The needle is insulated electrically, except at the point, with a resin varnish. A 1.5 volt battery and 10,000 ohm resistor are connected in series with the probe to ground; the conducting liquid is also grounded.

The principle of operation consists of the instantaneous measurement of local resistivity in the two-phase stream. When the needle tip is in contact with liquid the circuit is closed; when it is in contact with gas it is open. Since the series resistance is large compared to the probe resistance (approximately 10,000 to 1) the voltage drop across the series resistance will form a square wave of irregular frequency and constant amplitude of 1.5 volts. The break time was so small as to be nonmeasurable at a chart speed of about 2 ft./sec. This implies that, owing to the poor wetting of the probe tip by the mercury, no rounding of the corners of the square wave output could be observed.

Three important characteristics of the phase distribution can be determined from an analysis of the signal:

1. The frequency with which the phase changes at the probe tip. This may be identified with the local bubble frequency.
2. The fraction of time the circuit is open which is the local volumetric gas fraction.
3. The dwell time of each gas bubble. The following simplified analysis can be used to relate this quantity to the bubble diameter.*

If it is assumed that the bubbles are spherical with diameters small compared to the pipe diameter such that the bubbles move independently of the wall, then the probe has an equal probability of piercing any segment of projected bubble area. The median chord pierced will be at that cone angle which divides the projected bubble area into two parts, the probability of piercing each part being equal. Since the probability of piercing any increment of area is proportional to the size of the increment, the projected area of the bubble must be divided into a circle and an annular ring of equal area so that

$$\frac{\delta}{D_B} = \sqrt{\frac{1}{2}} \tag{6}$$

where δ is the diameter of the circular area. From simple geometric considerations it is also the median bubble chord pierced. δ is related to the dwell time, θ_B, by the bubble velocity, U_B

$$\delta = \theta_B U_B \tag{7}$$

Hence it follows that

$$D_B = \sqrt{2}\, \theta_B U_B \tag{8}$$

For very large bubbles ($\zeta \geq 1$) the measured length is coincident with the true length of the slug:

$$D_B = \theta_B U_B \tag{9}$$

Between these limiting conditions, very small and very large bubbles, there are many medium-size bubbles, and for these one may write

$$D_B = C\, \theta_B U_B \tag{10}$$

where $C = C(\zeta, S)$ is a parameter dependent upon the

* More sophisticated analyses are given in notes submitted to the *A.I.Ch.E. Journal* by T. T. Anderson and S. G. Bankoff.

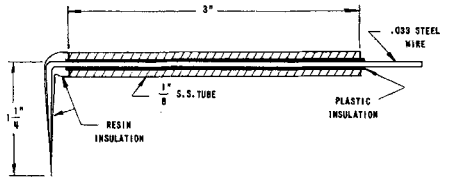

Fig. 1. Electrical resistivity probe.

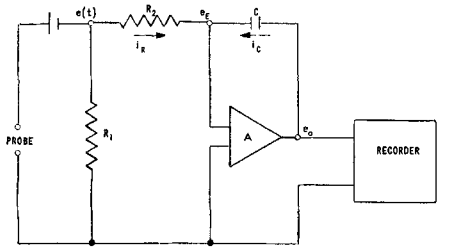

Fig. 2. Integrating circuit for determination of local void fraction.

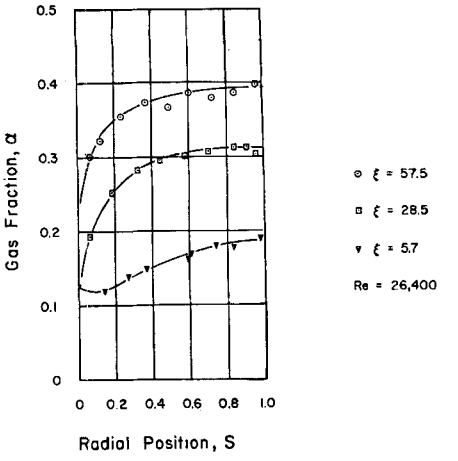

Fig. 3. Typical radial void fraction profiles at several axial positions.

bubble diameter and upon the radial position of the probe, since the probability that the probe will strike the bubble off-center increases as the wall is approached. It is thought, however, that this occurs only quite close to the wall, so that as an approximation one can assume that C varies linearly with bubble diameter independently of radial position: $C = \zeta + \sqrt{2}\,(1 - \zeta)$. The effect of this approximation will be to increase the apparent frequency of small bubbles near the wall.

ANALYSIS OF THE PROBE SIGNAL

An attempt was made to measure bubble frequency by means of a flip-flop circuit, which counts the number of times the voltage drops to zero with a digital counter. The response of the circuit was adequate to count a 100 cycles/sec. square-wave voltage correctly, but the bubble counts by this method were found to be considerably lower than those from the photographic record as detailed below. Bubble frequencies were therefore obtained by the latter method.

The dwell time for each bubble, θ_B, was determined by measuring the length of time the circuit was open with a photographic record of the probe signal. An oscillograph capable of recording signal frequencies to 2,000 cycles/sec. was used to record the signal.

The fraction of time the circuit was closed was determined by electronically integrating the signal for a time T. The integrating circuit is shown schematically in Figure 2. This is a standard circuit for which the following relationship holds:

$$e_0 = -\frac{1}{RC}\int_0^T \frac{e(t)}{E}\,dt \qquad (11)$$

A second integration was made with no gas flowing. The input signal was constant and equal to E so that the integral was $-\dfrac{ET}{RC}$. Dividing Equation (11) by this quantity gives

$$-e_0\frac{RC}{ET} = \frac{1}{T}\int_0^T \frac{e(t)}{E}\,dt = 1 - \alpha \qquad (12)$$

The quantity $e(t)/E$ possesses the properties of the function $\phi(t)$ as defined by Equation (5). After these data were taken an improved integrating circuit was developed which performs the division of Equation (11) by $-\dfrac{ET}{RC}$ electronically. Besides saving time, it allows $(1 - \alpha)$ to be recorded continuously. This gives new information about the minimum sample time interval necessary to measure α, and also about slow variations in the field of flow. In this improved circuit the output signals from two identical integrating circuits, the first integrating the fluctuating voltage $e(t)$, and the second integrating the constant voltage E, were fed to a function multiplier which divided the first integral by the second, resulting in a signal proportional to $1 - \alpha$:

$$e_0 = \frac{\dfrac{1}{RC}\displaystyle\int_0^T e(t)\,dt}{\dfrac{1}{RC}\displaystyle\int_0^T E\,dt} \qquad (13)$$

The amplifiers used in both integrating circuits had an output voltage range of ± 115 volts and gain of 10^7. The power supply was a compound regulated dual power supply with rated output at ± 300 volts. A strip chart recorder with 100 millivolt range was used to record the output signal. The circuit time constant, $RC = 2$ sec., allowed integration for 150 sec.

ILLUSTRATIVE EXAMPLE

The method may be considered for any gas-liquid, vapor-liquid or liquid-liquid system in which the continuous phase is an electrical conductor. It is, however, particularly advantageous for systems in which the continuous phase is a liquid metal because of the high electrical conductivity and high surface energy. The latter property results is poor wetting of the steel probe, so that a fast circuit break is obtained. For these reasons the probe was first used in a study of vertical cocurrent flow of a mercury-nitrogen mixture in a 1-in. stainless steel pipe. The flow system was a natural-circulation loop in which metered streams of mercury and nitrogen were fed to a mixer. The resulting two-phase stream entered the test section through a 150-mesh screen in order to obtain a more uniform initial gas distribution and bubble size. From the test section the mixture flowed into a separator where the nitrogen was vented to the atmosphere and the mercury returned by gravity flow to the mixer.

Profiles of the void fraction were measured at three positions along the length of the test section, at $\xi = 5.7$, 28.5, and 51.5, where $\xi = x/D_p$ is the axial position variable made dimensionless with reference to the pipe diameter. Complete data are given in (*15*). Figure 3 shows void fraction profiles for a typical experiment and demonstrates the gas distribution development as the flow develops. It is seen that $\dfrac{\partial\alpha}{\partial y} > 0$, where y is the distance

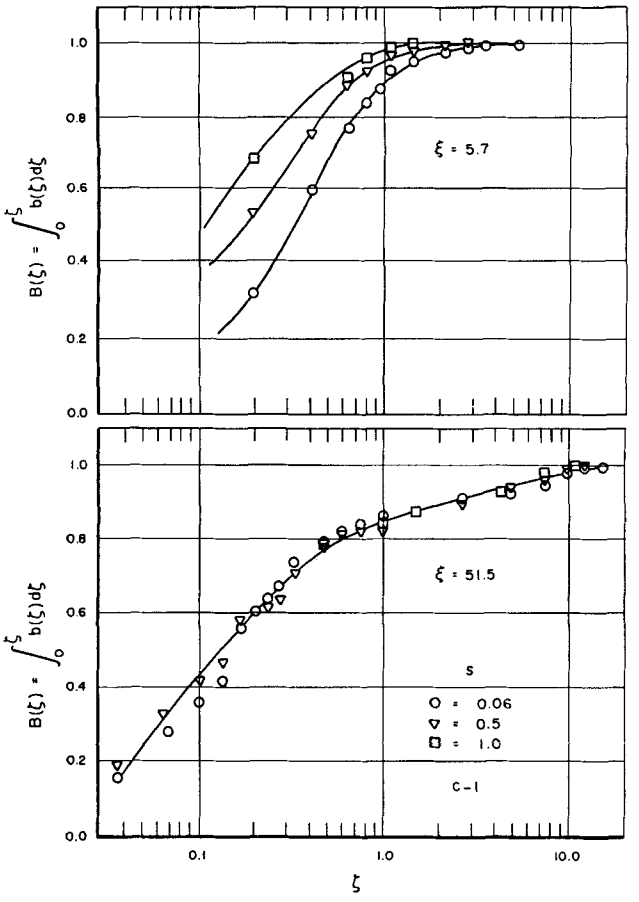

Fig. 4. Typical bubble diameter distribution functions at two axial positions.

from the tube wall, for $S = \frac{y}{R} << 1$ near the entrance of the test section ($\xi = 5.7$). This may be associated with the nonwetting property of the mercury. After the flow has developed further, at $\xi = 28.5$ and 51.5, the gas is forced to the center of the stream, giving a dome-shaped profile with a maximum at the center and decreasing rapidly near the wall. Records of the probe signal were taken at the same three positions along the length of the test section and at three radial positions, $S = 0.06$, 0.5, and 1.0. The bubble diameter distribution function, $B(\xi)$, can be computed from the distribution of dwell times with measurements of the local liquid velocity by a newly developed impact probe (*15*). Some of these results are shown in Figure 4 for $\xi = 5.7$ and 51.5. Near the entrance to the test section the bubble distribution function is generally weighted more at the center of the tube towards the smaller bubbles than near the wall. After the flow has become fully developed, the difference in distribution spectra is almost undistinguishable. The small bubbles are fairly uniformly distributed across the tube cross section. One may define higher-order moments $P_n(\zeta)$, of the bubble diameter distribution function, such that

$$P_n(\zeta) = \int_0^\zeta \zeta^n b(\zeta)\, d\zeta / \int_0^\infty \zeta^n b(\zeta)\, d\zeta \qquad (14)$$

assuming that the infinite integral converges. Then one observes from Figure 4 that $B(1) = P_0(1) = 0.85$, while $P_1(1)$, which is the contribution of such bubbles ($\zeta < 1$) to the measured gas fraction, is 0.031. $P_3(1)$, the volume fraction of gas contained in bubbles with $\zeta < 1$, is 0.0018. This is characteristic of slug flow. Although there is a greater number of small bubbles, most of the gas flow is carried by slugs.

The cumulative gas and liquid slug length distributions for fully developed flow are shown in Figure 5. Figure 6 shows bubble frequency data obtained from the oscillograph record. One sees that the frequency varies radially and axially in the entrance region, but becomes essentially constant when the flow is fully developed.

ERROR ANALYSIS

Since this is the first method capable of measuring point values of the flow parameters, there are no previous data with which to compare the results. However, it is possible to check the cross-section average void fraction obtained by integrating the local void fraction profile in the pipe with the average value obtained by some other method. One such method employs the measured static pressure profile along the pipe. From a consideration of the momentum equation, one finds that changes in the kinetic energy of the stream contribute less than 0.5% to the total static pressure loss and may be neglected. Similarly, the frictional loss is estimated by the method of Lockhart and Martinelli (*13*) to be less than 2% of the total static pressure loss and hence may be neglected.

The local pressure gradient is therefore very nearly equal to the mean density at the axial position

$$-\frac{dP}{dx} = \rho \qquad (15)$$

where the mixture density is defined by

$$\rho = (1 - \bar{\alpha})\, \rho_L + \bar{\alpha}\rho_G \qquad (16)$$

Noting that

$$\rho_G/\rho_L \simeq 1/4{,}000$$

one obtains

$$-\frac{dP}{dx} = (1 - \bar{\alpha})\, \rho_L \qquad (17)$$

When the pressure gradient along the test section is measured, values of $\bar{\alpha}$ can be calculated. Figure 7 shows the comparison of $\bar{\alpha}$ thus determined with values obtained by integrating a number of void fraction profiles to be reported elsewhere. One sees that the agreement is excellent with a maximum deviation of 0.06.

Errors owing to the electronic components were determined by replacing the probe signal with a square wave signal from a function generator. The integration circuit was found to integrate signals of 1,200 cycles/sec. with a maximum error equal to the error of reading the strip chart, ± 0.2 volts. Since two readings of the chart were required for each value of the gas fraction and the full chart range was used, the uncertainty in the gas fraction was less than ± 0.004.

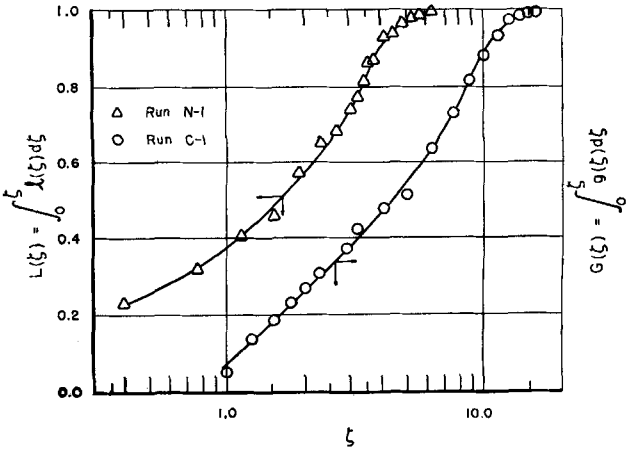

Fig. 5. Typical cumulative gas and liquid slug length distributions.

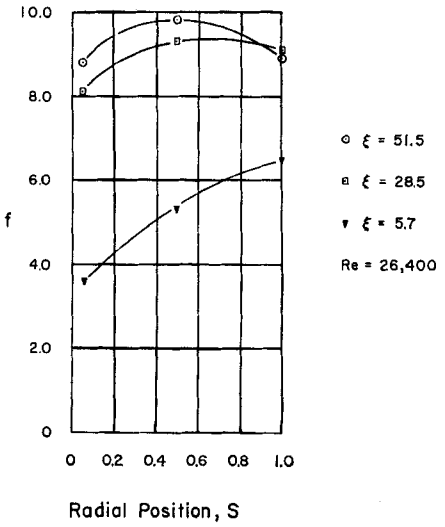

Fig. 6. Typical bubble frequencies at several axial and radial positions.

The response of the photographic recorder was fast enough to record the dwell time of every bubble pierced by the probe. The diameter of the probe tip was 0.02 in. and bubbles in this size range are probably deflected. However, because of the limit of chart speed, bubbles with $\theta_B = 0.003$ sec. (about 1/10 in.) and smaller appeared in the record as square waves of width 1/64 in. and less. It was not practical to differentiate between bubbles of this size, and they were all assigned a dwell time $\theta_B = 0.003$. The wave width for larger bubbles was measured to the nearest 1/64 in., so that the individual dwell times were accurate to $\pm$ 0.003 sec.

ACKNOWLEDGMENT

This work was sponsored by Argonne National Laboratory under the auspices of the Atomic Energy Commission. The cooperation and counsel of Dr. P. A. Lottes are gratefully acknowledged. Helpful discussions were also held with Dr. Helge Christensen of the Norwegian Institute of Atomic Energy and Professor F. A. Blanchard of the University of New Hampshire. Thanks are also due Albert Stogsdill who helped construct and operate the apparatus and reduce the data.

NOTATION

$B(\zeta)$ = bubble diameter distribution function
$b(\zeta)$ = density function for bubbles of diameter ζ
C = a constant, or electrical capacitance, farads
D_B = bubble diameter, ft.
D_p = pipe diameter, ft.
E = battery voltage, volts
e_o = output signal from integrating circuit, volts
$e(t)$ = fluctuating probe signal, volts
f = bubble frequency, bubbles/sec.
$G(\zeta)$ = gas slug length distribution function
$g(\zeta)$ = density length function for gas slugs
$L(\zeta)$ = liquid slug length distribution function
$l(\zeta)$ = density length function for liquid slugs
N = number of bubbles passing through given point in time T
P = pressure, lb./sq.ft. or probability
$P_n(\zeta)$ = bubble diameter moment distribution function, defined by Equation (14)
U_B = bubble velocity, ft./sec.
r = radial distance, ft.
R = pipe radius, ft. or electrical resistance, ohms
S = dimensionless distance from the tube wall, y/R
T = integration or counting time, sec.
t = time, sec.

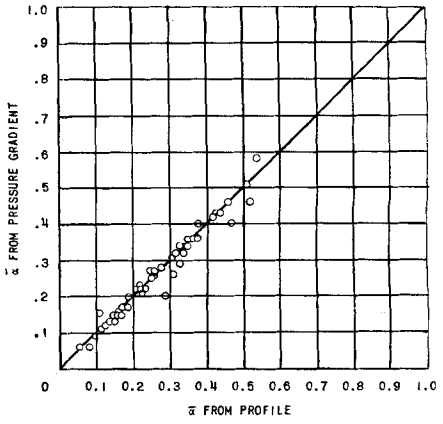

Fig. 7. Comparison of $\bar{\alpha}$ from static pressure gradient with $\bar{\alpha}$ by integration of probe local void fraction.

x = axial distance from entrance of test section, ft.
y = distance from the pipe wall, ft.

Greek Letters

α = point or local value of the void fraction
δ = average bubble chord length pierced by the probe, ft.
ζ = dimensionless bubble diameter, D_B/D_p, or slug length referred to the test section diameter
θ_B = time required for a bubble to pass the probe (dwell time), sec.
ξ = dimensionless axial distance from the test section inlet, x/D_p
ρ, ρ_G, ρ_L = density of the mixture, gas and liquid respectively, lb./cu.ft.
$\phi(t)$ = a discontinuous function of time which takes the value one when liquid exists at the probe tip and zero when gas exists at the probe tip

LITERATURE CITED

1. Hooker, H. H., and G. F. Popper, *Report No. 5766,* Argonne National Lab. (1958).
2. Petrick, M., *Report No. 5787,* Argonne National Lab. (1958).
3. Perkins, H. C., Jr., M. Yusuf, and G. Leppert, *Nucl. Sci. Eng.,* **11,** 304 (1961).
4. Dengler, C. E., Ph.D. thesis, Massachusetts Institute of Technology, Cambridge, Massachusetts (1952).
5. Griffith, Peter, J. A. Clark, and W. M. Rohsenow, *Am. Soc. Mech. Engrs. Paper 58-HT-19* (1958).
6. Johnson, H. A., and A. H. Abou-Sabe, *Trans. Am. Soc. Mech. Engrs.,* **74,** 977 (1952).
7. Egen, R. A., D. E. Dingee, and J. W. Chastain, *Report No. 1163,* Battelle Memorial Institute (1957).
8. Cook, W. H., *Report No. 5621,* Argonne National Lab. (1956).
9. Krasiakova, L. I., *Zhur. Tech. Fiz.,* **22,** 4, 656 (1952).
10. McManus, H. N., *Am. Soc. Mech. Engrs. Paper 57-A-144,* (1958).
11. Hewitt, G. F., R. D. King, and P. C. Lovegrove, *Report No. 3921,* Atomic Energy Research Establishment, Harwell, England (1961).
12. Solomon, J. V., M.S. thesis, Massachusetts Institute of Technology, Cambridge, Massachusetts (1962).
13. Lockhart, R. W., and R. C. Martinelli, *Chem. Eng. Progr.,* **45,** 39 (1949).
14. Petrick, M., *Report No. 6581,* Argonne National Lab. (1962).
15. Neal, L. G., Ph.D. thesis, Northwestern University, Evanston, Illinois (1962); *Report No. 6625,* Argonne National Lab. (1963).

Manuscript received September 28, 1962; revision received January 2, 1963; paper accepted January 4, 1963. Paper presented at A.I.Ch.E. Chicago meeting.